

# Coupled cluster approach to nuclear physics

D. J. Dean

*Physics Division, Oak Ridge National Laboratory, P.O. Box 2008, Oak Ridge, TN 37831-6373*

M. Hjorth-Jensen

*Department of Physics and Center of Mathematics for Applications, University of Oslo, N-0316 Oslo, Norway*

(Dated: November 2, 2018)

Using many-body perturbation theory and coupled-cluster theory, we calculate the ground-state energy of  ${}^4\text{He}$  and  ${}^{16}\text{O}$ . We perform these calculations using a no-core  $G$ -matrix interaction derived from a realistic nucleon-nucleon potential. Our calculations employ up to two-particle-two-hole coupled-cluster amplitudes.

## I. INTRODUCTION

The coupled-cluster method originated in nuclear physics over forty years ago when Coester and Kummel proposed an exponential ansatz to describe correlations within a nucleus [1, 2]. This ansatz has been well justified for many-body problems using a formalism in which the cluster functions are constructed by cluster operators acting on a reference determinant [3]. Early applications to finite nuclei were described in Ref. [4]. From that time to this, a systematic development and implementation of this interesting many-body theory in nuclear physics applications has been only sporadic. The view from computational quantum chemistry is quite different. In fact, coupled-cluster methods applied to computational chemistry enjoy tremendous success [5, 6, 7, 8, 9, 10] over a broad class of chemistry problems related to chemical and molecular structure and chemical reactions.

Many solid theoretical reasons exist that motivate a pursuit of coupled-cluster methods. First of all, the method is fully microscopic and is capable of systematic and hierarchical improvements. Indeed, when one expands the cluster operator in coupled-cluster theory to all  $A$  particles in the system, one exactly produces the fully-correlated many-body wave function of the system. The only input that the method requires is the nucleon-nucleon interaction. The method may also be extended to higher-order interactions such as the three-nucleon interaction. Second, the method is size extensive which means that only linked diagrams appear in the computation of the energy (the expectation value of the Hamiltonian) and amplitude equations. As discussed in Ref. [6] all shell model calculations that use particle-hole truncation schemes actually suffer from the inclusion of unconnected diagrams in computations of the energy. Third, coupled-cluster theory is also size consistent which means that the energy of two non-interacting fragments computed separately is the same as that computed for both fragments simultaneously. In chemistry, where the study of reactions is quite important, this is a crucial property not available in the interacting shell model (named configuration interaction in chemistry). Fourth, while the theory is not variational, the energy behaves as a variational quantity in most instances. Finally, from a com-

putational point of view, the practical implementation of coupled cluster theory is amenable to parallel computing.

Applications to nuclear problems resurfaced a few years ago in the works of Mihalia and Heisenberg [11, 12, 13, 14]. These efforts focused primarily on the structure of  ${}^{16}\text{O}$ , and used a strategy of solution that is somewhat different from the approach we will take in this and subsequent articles. One major difference is that we will use a  $G$ -matrix to renormalize the two-body interactions before we begin our coupled-cluster calculations. We will also take a somewhat different approach in our Hilbert space truncation. Also notable is the work of Moliner, Walet, and Bishop [15] who are pursuing nuclear problems in translationally invariant coupled cluster methods in coordinate space.

The computed energy using the coupled-cluster formalism includes a very large class of many-body perturbation theory diagrams. In standard many-body perturbation theory, one typically sums all diagrams order by order. The coupled-cluster approach essentially iterates diagrams so that one may discuss it in terms of an infinite summation of particular classes of diagrams. Thus the theory is nonperturbative. In fact the coupled-cluster energy at the single and double excitation level contains contributions identical to those of second order and third order many-body perturbation theory, but lacks triple excitation contributions necessary to complete fourth-order many-body perturbation theory; see e.g., the review article of Bartlett [5]. It has been shown that the quadruple excitation contributions may be factored exactly into products of double excitations, but no such factorization is possible for the corresponding triples. Therefore, the coupled-cluster energy lacks only triple excitation contributions to be complete through fourth order.

In this paper, we wish to establish a line of research that we intend to pursue for calculating nuclear properties using coupled-cluster techniques. This is therefore a first paper in a series that we will publish to both develop the method for nuclear physics and to demonstrate the power of the method for various applications. This first installment will be devoted to outlining our approach, investigating the physical motivations, establishing numerical convergence tests, and presenting some initial calculations using the method. In Sec. II, we will

describe our choice of reduced Hilbert space, construction of an effective interaction for various model spaces and elimination of the spurious center of mass motion. The model spaces are defined in terms of various major harmonic oscillator shells and the effective interaction is defined in terms of the  $G$ -matrix, see e.g., Ref. [16]. Our calculations of the binding energy of nuclei like helium and oxygen entail therefore a dependence upon the number of harmonic oscillator states, the oscillator parameter and the starting energy at which the  $G$ -matrix is computed. The convergence of the binding energy as function of the number of harmonic oscillator shells is a crucial test of the method discussed in this work. Since the coupled-cluster calculations are rather time consuming for systems like  $^{16}\text{O}$ , we present, as an introduction to the coupled-cluster method, intermediate results from perturbative many-body approaches in Sec. III. Sec. III also serves the purpose of finding an eventual minimum for the energy as function of the oscillator parameter, with which we limit the number of coupled-cluster computations. It may also be of help in finding how many oscillator shells are needed in order to achieve a satisfactory convergence. In addition, this section sheds lights on the limitations of many-body perturbation theory compared with the coupled-cluster approach.

We turn in Sec. IV to a description of the coupled-cluster equations. We discuss the numerical techniques we will employ to obtain solutions to the coupled-cluster equations and demonstrate several results for  $^4\text{He}$  and  $^{16}\text{O}$  in Sec. V. We conclude with a prospective for future directions of this research in Sec. VI.

## II. EFFECTIVE INTERACTIONS FOR A TRUNCATED HILBERT SPACE

The aim of this section is to present and partly justify the computation of an effective two-body Hamiltonian acting within a reduced Hilbert space. This two-body Hamiltonian will in turn serve as the starting point for the perturbative approach of Sec. III and the coupled-cluster expansion discussed in Sec. IV.

Before we can compute such an effective two-body Hamiltonian, we need to define the nucleon-nucleon interaction. Several types of modern nucleon-nucleon scattering interactions have been developed during recent years. These interactions all fit nucleon-nucleon scattering data up to 300 MeV with excellent precision [17, 18, 19]. They do give slightly differing results for the radius of the deuteron, the binding energy of the triton and also contain slight differences in the way they treat locality.

Very recent work by Entem and Machleidt [20] provides for the first time an interaction of quantitative accuracy that is based on effective field theory. One basic open question of nuclear theory involves understanding how the nucleon-nucleon interaction may be derived from quantum chromodynamics, the theory of strong interactions. Quantum chromodynamics has not been solved in

its nonperturbative low-energy limit at energy scales that are characteristic for low-energy nuclear physics. One promising way to circumvent this problem is to employ a derivation of the nuclear force based on chiral effective field theory [21, 22]. The authors of Ref. [20] undertook the task of generating an accurate nucleon-nucleon interaction based on chiral perturbation theory. They included one- and two-pion exchange contributions up to chiral order three. They also showed that a quantitative fit of the nucleon-nucleon  $D$ -wave phase shifts requires contact terms representing short-range forces of order four. The number of free parameters used in this chiral interaction is 46, which is similar to the number of free parameters found in other two-nucleon forces. The phase-shift analysis shows excellent agreement between the chiral interaction and the scattering data.

Two interactions were formulated in Ref. [20]. These two models, denoted Idaho-A and Idaho-B, differ in their prediction of the  $D$ -state probabilities of the deuteron, while both interactions will give the same values for the  $^3S_1$ ,  $^3D_1$  and  $\epsilon_1$  phase parameters up to 300 MeV in scattering energy. Idaho-A yields a  $D$ -state probability of 4.17%, while Idaho-B gives 4.94%. This also affects the triton binding energy, yielding 8.14 MeV and 8.02 MeV for Idaho-A and Idaho-B, respectively. A similar interaction which now goes to fourth order in chiral perturbation theory and includes charge dependence, has recently been presented by Entem and Machleidt, see Ref. [23]. Since this is a methodological paper, we limit the attention to one of these interactions, namely the Idaho-A model. Results for other interactions, such as the  $V_{18}$  model of the Argonne group [18], will be presented in future work.

### A. Definition of the model space and the two-body effective interaction

In order to derive an effective interaction suitable for coupled cluster calculations, we need to introduce various notations and definitions pertinent to the methods exposed.

A common practice in nuclear many-body theory is to reduce the infinitely many degrees of freedom of the Hilbert space to those represented by a physically motivated subspace, the model space. In such truncations of the Hilbert space, the notions of a projection operator  $P$  onto the model space and its complement  $Q$  are introduced. The projection operators defining the model and excluded spaces are

$$P = \sum_{i=1}^D |\Phi_i\rangle \langle \Phi_i|, \quad (1)$$

and

$$Q = \sum_{i=D+1}^{\infty} |\Phi_i\rangle \langle \Phi_i|, \quad (2)$$

with  $D$  being the dimension of the model space, and  $PQ = 0$ ,  $P^2 = P$ ,  $Q^2 = Q$  and  $P + Q = I$ . The two-body wave functions  $|\Phi_i\rangle$  are normally eigenfunctions of an unperturbed Hamiltonian  $H_0$ . In this work we let only the kinetic energy enter the definition of  $H_0$ , i.e.,  $H_0 = t$ . Since we will employ a harmonic oscillator basis, this means that we need to compute the expectation value of  $H_0$  as well. The unperturbed wave functions are not eigenfunctions of  $t$ . The full Hamiltonian is then  $H = t + V_{NN}$  with  $V_{NN}$  the nucleon-nucleon interaction. The eigenfunctions of the full two-body Hamiltonian are denoted by  $|\Psi_\alpha\rangle$  and  $E_\alpha$ ,

$$H|\Psi_\alpha\rangle = E_\alpha|\Psi_\alpha\rangle. \quad (3)$$

Rather than solving the full Schrödinger equation above, we define an effective Hamiltonian acting within the model space such that

$$PH_{\text{eff}}P|\Psi_\alpha\rangle = E_\alpha P|\Psi_\alpha\rangle = E_\alpha|\Phi_\alpha\rangle \quad (4)$$

where  $|\Phi_\alpha\rangle = P|\Psi_\alpha\rangle$  is the projection of the full wave function onto the model space, the model space wave function. Here  $H_{\text{eff}}$  is an effective Hamiltonian acting solely within the chosen model space given by  $H_{\text{eff}} = PtP + V_{\text{eff}}$ , with the interaction

$$V_{\text{eff}} = \sum_{i=1}^{\infty} V_{\text{eff}}^{(i)}, \quad (5)$$

where  $V_{\text{eff}}^{(1)}$ ,  $V_{\text{eff}}^{(2)}$ ,  $V_{\text{eff}}^{(3)}$ , ... are effective one-body, two-body, three-body interactions etc. For finite  $A$ -body systems, the sum terminates at  $i = A$ . As stated above, in this work we will limit the attention to two-body interactions. The next step could be to employ perturbative many-body techniques or the coupled cluster method. In perturbation theory, the effective interaction  $H_{\text{eff}}$  can be written out order by order in the interaction  $V_{NN}$  as

$$PH_{\text{eff}}P = PtP + PV_{NN}P + PV_{NN}\frac{Q}{e}V_{NN}P + PV_{NN}\frac{Q}{e}V_{NN}\frac{Q}{e}V_{NN}P + \dots \quad (6)$$

In this expansion,  $e = \omega - t$ , where  $\omega$  is the so-called starting energy, defined as the unperturbed energy of the interacting particles. However, the nucleon-nucleon interactions all possess a hard core that makes them unsuitable for perturbative many-body approaches. The standard procedure is therefore to renormalize the short-range part of the interaction by introducing the so-called reaction matrix  $G$

$$G = V_{NN} + V_{NN}\frac{\tilde{Q}}{\omega - \tilde{Q}t\tilde{Q}}G. \quad (7)$$

The operator  $\tilde{Q}$  is normally different from the projection operator defined in Eq. (2), since the  $G$ -matrix by construction allows only specific two-body states to be defined by  $\tilde{Q}$ . Typically, the  $G$ -matrix is the sum over all ladder type of diagrams with intermediate particle-particle states only. This sum is meant to renormalize the repulsive short-range part of the interaction. The physical interpretation is that the particles must interact with each other an infinite number of times in order to produce a finite interaction. This interaction can in turn serve as an effective interaction acting in a reduced space.

We illustrate the definition of the exclusion operator employed in this work in Fig. 1. Using a harmonic oscillator basis for the single-particle wave functions, a single-particle state is classified by the quantum numbers  $nlj$ . A two-particle state in an angular momentum coupling scheme is given by  $|(n_\alpha l_\alpha j_\alpha n_\beta l_\beta j_\beta)JT_Z\rangle$ , where  $\alpha$  and  $\beta$  represent one of the orbitals  $0s_{1/2}$ ,  $0p_{3/2}$ ,  $0p_{1/2}$  etc and  $J$  is the total two-particle angular momentum and  $T_Z$  the

corresponding isospin projection.

The single-particle states labeled by  $n_1 l_1 j_1$  and  $n_2 l_2 j_2$  represent the last orbit of model space  $\tilde{P}$ . In this work  $n_1 l_1 j_1$  and  $n_2 l_2 j_2$  will mark the number of harmonic oscillator shells included in the definition of  $\tilde{P}$ . In the actual calculations presented below these range from four to eight major shells. For four major shells  $n_1 l_1 j_1 = 2s_{1/2}$  and  $n_2 l_2 j_2 = 2s_{1/2}$  while for eight major shells we get  $n_1 l_1 j_1 = 3p_{1/2}$  and  $n_2 l_2 j_2 = 3p_{1/2}$  as the last single-particle orbits. In Fig. 1 the two-body state  $|(n_\alpha l_\alpha j_\alpha n_\beta l_\beta j_\beta)JT_Z\rangle$  does not belong to the model space and is included in the computation of the  $G$ -matrix. Similarly,  $|(n_\alpha l_\alpha j_\alpha n_\gamma l_\gamma j_\gamma)JT_Z\rangle$  and  $|(n_\delta l_\delta j_\delta n_\beta l_\beta j_\beta)JT_Z\rangle$  also enter the definition of  $\tilde{Q}$  whereas  $|(n_\delta l_\delta j_\delta n_\gamma l_\gamma j_\gamma)JT_Z\rangle$  is not included in the computation of  $G$ . This means that correlations not defined in the  $G$ -matrix need to be computed by other non-perturbative resummations or many-body schemes. This is where the coupled-cluster scheme enters.

Before we proceed we outline the computation of the  $G$ -matrix using the exclusion operator of Fig. 1. One can solve the equation for the  $G$ -matrix for finite nuclei by employing a formally exact technique for handling  $\tilde{Q}$  discussed in e.g., Ref. [16]. Using the matrix identity, for which  $\tilde{P}$  is the complement of  $\tilde{Q}$  such that  $\tilde{P} + \tilde{Q} = 1$ ,

$$\tilde{Q}\frac{1}{\tilde{Q}e\tilde{Q}}\tilde{Q} = \frac{1}{e} - \frac{1}{e}\tilde{P}\frac{1}{\tilde{P}e^{-1}\tilde{P}}\tilde{P}\frac{1}{e}, \quad (8)$$

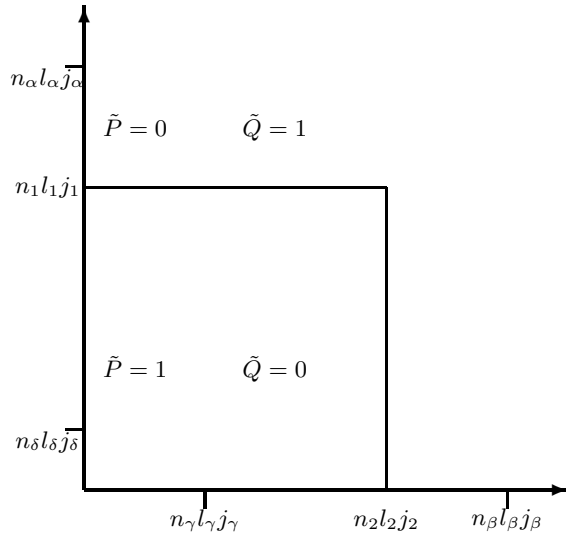


FIG. 1: Definition of the exclusion operator used to compute the  $G$ -matrix. See text for further details.

to rewrite Eq. (7) as

$$G = G_F + \Delta G, \quad (9)$$

where  $G_F$  is the free  $G$ -matrix defined as

$$G_F = V_{NN} + V_{NN} \frac{1}{\omega - t} G_F. \quad (10)$$

The term  $\Delta G$  is a correction term defined entirely within the model space  $\tilde{P}$  and given by

$$\Delta G = -V_{NN} \frac{1}{A} \tilde{P} \frac{1}{\tilde{P} A^{-1} \tilde{P}} \tilde{P} \frac{1}{A} V_{NN}. \quad (11)$$

Employing the definition for the free  $G$ -matrix of Eq. (10), one can rewrite the latter equation as

$$\Delta G = -G_F \frac{1}{e} \tilde{P} \frac{1}{\tilde{P} (e^{-1} + e^{-1} G_F e^{-1}) \tilde{P}} \tilde{P} \frac{1}{e} G_F, \quad (12)$$

with  $e = \omega - t$ . We see then that the  $G$ -matrix is expressed as the sum of two terms; the first term is the free  $G$ -matrix with no corrections included, while the second term accounts for medium modifications due to the exclusion operator  $\tilde{Q}$ . The second term can easily be obtained by some simple matrix operations involving the model-space matrix  $\tilde{P}$  only. The above allows, for a given model space operator  $\tilde{P}$ , for a numerically exact computation of the  $G$ -matrix.

The  $G$ -matrix defined by the exclusion operator  $\tilde{Q}$  of Fig. 1 represents now our effective two-body interaction, with a reduced Hilbert space defined by the model space  $\tilde{P}$ . This means that our Hamiltonian acts within the model space  $\tilde{P}$  and is given by

$$H_{\text{eff}}(\omega) = t + G(\omega). \quad (13)$$

The results from exact shell-model diagonalizations, perturbative many-body calculations and coupled-cluster calculations will depend on the limits of the model space  $\tilde{P}$  and the chosen oscillator parameter. Furthermore, although the  $G$ -matrix has a weak dependence upon the starting energy  $\omega$ , this dependence will affect the final results the calculations. The dependence of the results upon these parameters will be elucidated in Secs. III and V.

We end this subsection with the setup of the exclusion operator used in the final perturbative many-body calculations of Sec. III and the coupled cluster calculations of Sec. V.

With the  $G$ -matrix model space  $\tilde{P}$  of Fig. 1 we can now define an appropriate space for many-body perturbation theory and coupled-cluster calculations where correlations not included in the  $G$ -matrix are to be generated. This model space is defined in Fig. 2, where the labels  $n_{p,q} l_{p,q} j_{p,q}$  represent the same single-particle orbits as  $n_{1,2} l_{1,2} j_{1,2}$  in Fig. 1. Hereafter we use the notation that  $p, q, r, s$  index all single-particle states, while  $i, j, k, l$  refer to single-hole states

The  $G$ -matrix does not reflect a specific nucleus and thereby single-particle orbits which define the uncorrelated Slater determinant. For a nucleus like  ${}^4\text{He}$  the  $0s_{1/2}$  orbit is fully occupied and defines thereby single-hole states. These are labeled by  $n_i l_i j_i$  in Fig. 2. For  ${}^{16}\text{O}$  the corresponding hole states are represented by the orbits  $0s_{1/2}$ ,  $0p_{3/2}$  and  $0p_{1/2}$ . With this caveat we can then generate correlations not included in the  $G$ -matrix.

The unperturbed Hamiltonian  $H_0$  is given by the kinetic energy only. However, in order to define a suitable starting point for an effective interaction to be used in the coupled-cluster calculations we use the definition of particles and holes in Fig. 2 and compute the single-hole energies  $\varepsilon_i$  through

$$\varepsilon_i = \langle i | \frac{p^2}{2m} | i \rangle + \sum_{j \leq F} \langle ij | G(\omega = \varepsilon_i + \varepsilon_j) | ij \rangle, \quad (14)$$

where  $F$  stands for the Fermi energy. We do not perform a self-consistent Brueckner-Hartree-Fock calculation however, as done by e.g., Gad and Mütter [24], the reason being that this self-consistency is taken care of by the coupled-cluster procedure. The matrix elements are all antisymmetrized. Furthermore, for single-particle states above the Fermi energy we leave the single-particle energies unchanged. This procedure, which follows the Bethe-Brandow-Petschek theorem [25], introduces an artificial gap at the Fermi surface. Note also that the single-particle wave functions are not changed in Eq. (14). The main purpose of the above procedure is to yield a prescription for obtaining a starting energy independent effective interaction for the coupled-cluster calculations. Using the single-particle energies from Eq. (14) we define, following Ref. [24], an effective interaction for our coupled-cluster model spaces by

$$\langle ij | \mathcal{V}_{\text{eff}} | kl \rangle = \frac{1}{2} [\langle ij | G(\omega = \varepsilon_i + \varepsilon_j) | kl \rangle$$

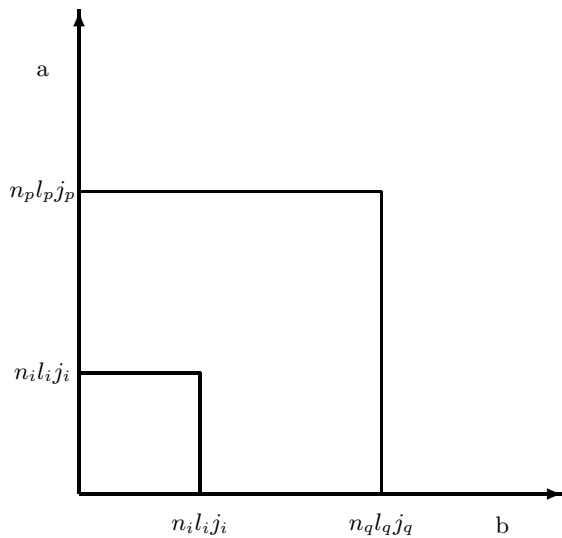


FIG. 2: Definition of particle and hole states for coupled-cluster and perturbative many-body calculations. We use the notation that  $p, q, r, s$  index all single-particle states, while  $i, j, k, l$  refer to single-hole states. The orbits represented by the quantum numbers  $n_i l_i j_i$  represent hole states whereas  $n_p, q l_p, q j_p, q$  represent the last particle orbits included in the  $G$ -matrix model space. The hole states define the Fermi energy.

$$+ \langle ij | G(\omega = \varepsilon_k + \varepsilon_l) | kl \rangle, \quad (15)$$

for two-body states with holes only and

$$\langle ip | \mathcal{V}_{\text{eff}} | kq \rangle = \frac{1}{2} [\langle ip | G(\omega = \varepsilon_i + \varepsilon_p) | kq \rangle + \langle ip | G(\omega = \varepsilon_k + \varepsilon_q) | kq \rangle], \quad (16)$$

for two-body states with one particle and one hole. For two-body states with two single-particle states  $pq$  we use a fixed starting energy, typically in the range  $\omega \in [-80, -5]$  MeV. This introduces a starting energy dependence in our results. The reason for fixing the starting energies for two-particle states is due to the fact that we use kinetic energies only above the Fermi surface and our  $G$ -matrices are computed at negative starting energies only.

An obvious improvement to this procedure is to generate a complex  $G$ -matrix which takes care of both positive and negative energies, reflecting thereby the non-resonant continuum, bound two-body states and eventual resonances and/or virtual states. We will however leave this interesting topic to a further study. The main focus of this paper is to establish a method for doing the coupled-cluster calculations without having to resort to employing the bare interaction, needing thereby many major harmonic oscillator shells. Our hope is that with a  $G$ -matrix, 7 – 8 major shells may suffice. Such a truncation in the harmonic oscillator space is supported by the

recent works of Barrett, Navratil, and Vary [26, 27, 28], see also the recent calculations of Ref. [29]. In these works no-core shell-model calculations have been mounted for light nuclei ranging from the triton to mass  $A = 12$ . Furthermore, in Refs. [26, 27], another approach for obtaining a starting energy independent interaction is obtained through the similarity transformations of Lee and Suzuki [30, 31], yielding a fully hermitian effective interaction. This should be contrasted to the more approximate method presented in Eqs. (15) and (16).

## B. Treatment of center-of-mass motion

Momentum conservation requires that a many-body wave function must factorize as  $\Psi(\mathbf{r}) = \phi(\mathbf{R})\Psi(\mathbf{r}_{\text{rel}})$  where  $R$  is the center-of-mass coordinate and  $\mathbf{r}_{\text{rel}}$  the relative coordinates. If we choose to expand our wave functions in the harmonic oscillator basis, then we are able to exactly separate the center-of-mass motion from the problem provided that we work in a model space that includes all  $n\hbar\omega$  excitations. In this paper, we perform calculations with a  $Q$  operator that allows for all possible two-particle interactions within a given set of oscillator shells. This means that we are  $n\hbar\omega$  incomplete in a given calculation so that our method of separation of the center-of-mass motion becomes approximate. For example, for  ${}^4\text{He}$  in four major oscillator shells, we can excite all particles to  $n = 12\hbar\omega$  excitations, but we can only excite one particle to  $n = 3\hbar\omega$  excitations. Thus, care must be taken when correcting for center-of-mass contamination in our calculations. We have taken a variational approach based on the the work of Whitehead *et al.*, [32]. The idea is to add  $\beta_{\text{c.m.}} H_{\text{c.m}}$  to the Hamiltonian, but with  $\beta_{\text{c.m.}}$  remaining fairly small. This minimizes the effects of the center-of-mass contamination on low-lying state properties, and partially pushes unwanted states out of the spectrum. If we were to use a large  $\beta_{\text{c.m.}}$ , we would find spurious states entering into the calculated low-lying spectrum due to the incompleteness of our model space.

We proceed as follows. The center-of-mass Hamiltonian is

$$H_{\text{c.m.}} = \frac{\mathbf{P}^2}{2MA} + \frac{1}{2}m A \omega^2 \mathbf{R}^2 - \frac{3}{2}\hbar\omega, \quad (17)$$

where  $\mathbf{P} = \sum_{i=1,A} \mathbf{p}_i$  and  $R = (\sum_{i=1,A} \mathbf{r}_i)/A$ .  $H_{\text{c.m.}}$  can be rewritten as a one-body harmonic potential, and a two-body term that depends on both the relative and center-of-mass coordinates of the two interacting particles. The matrix elements for the two body terms may be found in Ref. [33]. Operationally, we add  $H_{\text{c.m}}$  to our Hamiltonian

$$H' = H + \beta_{\text{c.m.}} H_{\text{c.m.}}, \quad (18)$$

where we choose  $\beta_{\text{c.m.}}$  so that the expectation value of  $H_{\text{c.m}}$  is zero [34]. This insures that our center-of-mass contamination within the many-body wave function is

minimized. We also find that this procedure yields reasonable spectra (in a space of four major oscillator shells) for  $^4\text{He}$  [35].

### III. PERTURBATIVE MANY-BODY METHODS

Our results will depend on the size of the model space and the chosen harmonic oscillator energy  $\hbar\omega$ . This section serves therefore two aims central to the coupled-cluster approach of this work.

- In the coupled-cluster calculations we search for an energy minimum as function of e.g., the oscillator energy  $\hbar\omega$ . Even for small systems like  $^{16}\text{O}$  with five or six major shells included, these are major time-consuming calculations. Results from many-body perturbation theory, which to second or third order in the interaction  $G$  are fairly simple, may therefore serve as a guide in order to limit the range of  $\hbar\omega$  values used in the coupled-cluster calculations. With increasing dimensionality of the  $G$ -matrix model space, the results should become independent of the oscillator energy.
- The energy will also depend on the size of the model space. The hope is that not too many shells are needed in order to achieve a converged energy. With the present approach, our coupled-cluster calculations of  $^{16}\text{O}$  are limited to six major shells. Results from many-body perturbation theory can thus serve as a guideline.

The linked-diagram theorem [10, 36] can be used to obtain a perturbative expansion for the energy in terms of the perturbation  $V(G)$  or  $V = H - H_0$  where  $H_0$  represents the unperturbed part of the Hamiltonian. The expression for the energy  $E$  reads

$$E = \sum_{k=0}^{\infty} \langle \Psi_0 | H [(\omega - H_0)^{-1} H]^k | \Psi_0 \rangle_L, \quad (19)$$

where  $\Psi_0$  is the uncorrelated Slater determinant for the ground state,  $\omega$  is the corresponding unperturbed energy and the subscript  $L$  stands for linked diagrams only. In

our calculations, we must replace the Hamiltonian  $H$  with the effective one defined in Eq. (13) and employ the definition of particle and hole states of Fig. 2. In Fig. 3 we show all antisymmetrized Goldstone diagrams through third order in perturbation theory (we omit the first order diagram). All closed circles stand for a summation over hole states. In this section we let the  $G$ -matrix define the interaction vertex. Since we do not use a self-consistently determined single-particle Hamiltonian, we need to account for diagrams with so-called Hartree-Fock insertions as well. Examples of the latter are shown in Fig. 3, see also the work of Kassis [37] for a detailed discussion of the various diagrams. There is an additional problem with our many-body perturbation

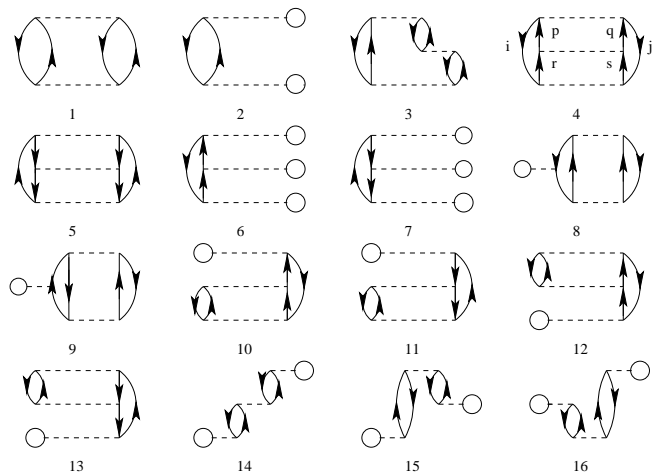


FIG. 3: Antisymmetrized Goldstone diagrams through third order in perturbation theory included in the evaluation of the binding energy. The dashed lines represents the interaction, in our case the  $G$ -matrix. Particle and hole states are represented by upward and downward arrows, respectively. The first order diagram is omitted. All closed circles stand for a summation over hole states.

theory calculations. Consider the expression  $\Delta E_4$  for diagram 4 in an angular momentum coupled basis (with  $J$  being the total two-body angular momentum and  $T_z$  the corresponding isospin projection) of Fig. 3

$$\Delta E_4 = \frac{1}{8} \sum_{\substack{ij \leq F \\ pqrs > F \\ J}} (2J+1) \langle (ij)JT_z | G(\omega = \varepsilon_i + \varepsilon_j) | (pq)JT_z \rangle \frac{1}{\varepsilon_i + \varepsilon_j - \varepsilon_p - \varepsilon_q} \times \langle (pq)JT_z | G(\omega = \varepsilon_i + \varepsilon_j) | (rs)JT_z \rangle \frac{1}{\varepsilon_i + \varepsilon_j - \varepsilon_r - \varepsilon_s} \langle (rs)JT_z | G(\omega = \varepsilon_i + \varepsilon_j) | (ij)JT_z \rangle. \quad (20)$$

The  $G$ -matrices depend on the starting energy  $\omega$ , defined in this case by the hole energies. With a harmonic os-

illator basis and with kinetic energies only these start-

ing energies will be positive, whereas our  $G$ -matrix is defined for negative energies only with  $\omega \in [-140, -5]$  MeV. To remove this problem we employ the single-hole energies computed according to Eq. (14). This leads to an artificial gap at the Fermi surface and demonstrates one of the problems with many-body perturbation theory. A self-consistent approach is needed both for holes and particles, and the  $G$ -matrix needs to be computed for both positive and negative energies. This is however beyond the scope of this work, where our emphasis is on the coupled-cluster approach. The center-of-mass corrections discussed in the previous section are not included in our perturbative calculations. This section, as will be seen below, serves the main aim of justifying our model space used in the coupled-cluster computation. In addition, the energy minimum as function of the oscillator energy limits the range of  $\hbar\omega$  values used in the coupled-cluster calculations.

Needless to say, many-body perturbation theory has severe limitations. It is very difficult to go beyond third order in perturbation theory without a self-consistent single-particle potential and beyond fourth order with a self-consistent potential. The coupled-cluster method offers on the other hand a systematic way to generate all many-body correlations in a given model space.

#### A. Many-body perturbation theory results for helium and oxygen

We present here results from third-order in perturbation theory for the binding energies of  ${}^4\text{He}$  and  ${}^{16}\text{O}$  as functions of the size of the model space and the chosen oscillator energy  $\hbar\omega$ . These results are shown in Figs. 4 and 5 for  ${}^4\text{He}$  and  ${}^{16}\text{O}$ , respectively.

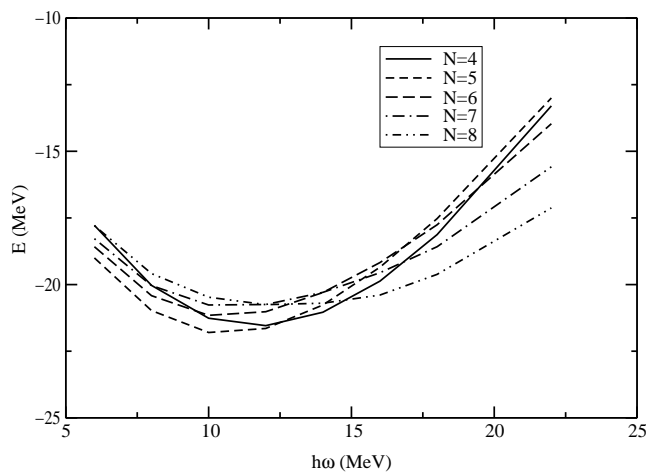


FIG. 4: Binding energy  $E$  from third-order perturbation theory for  ${}^4\text{He}$  as function of the number of major harmonic oscillator shells  $N$  and the oscillator energy  $\hbar\omega$ . For  $N = 8$  we have the optimal value of  $E = -20.830$  MeV at  $\hbar\omega = 13.3$  MeV. The experimental value is  $E = -28$  MeV.

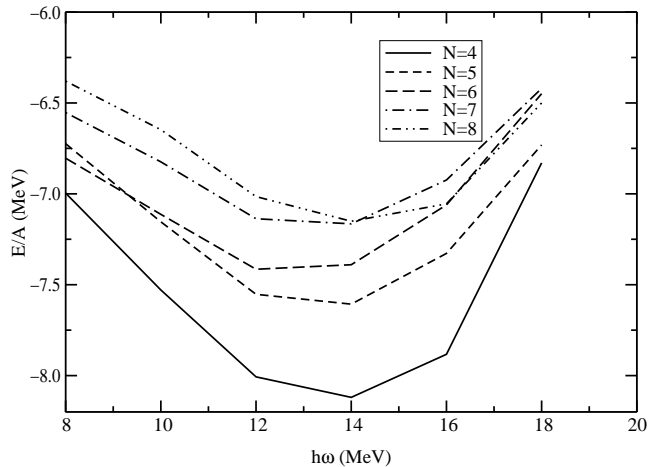


FIG. 5: Binding energy per particle  $E/A$  from third-order perturbation theory for  ${}^{16}\text{O}$  as function of the number of major harmonic oscillator shells  $N$  and the oscillator energy  $\hbar\omega$ . For  $N = 8$  we have the optimal value of  $E/A = -7.120$  MeV at  $\hbar\omega = 13.6$  MeV. The experimental value is  $E/A = -7.98$  MeV.

There are several features to be noted. First of all, both figures show that the results seem to stabilize between seven and eight major shells. For  ${}^4\text{He}$  all possible excitations within these shells are allowed in the computation of the diagrams, to be contrasted to the work of Kassis [37] and other traditional approaches [16] where one typically considers only  $2 - 4\hbar\omega$  excitations. For  ${}^{16}\text{O}$  we keep the same numbers of maximum allowed excitations for both the  $0s_{1/2}$  shell and the  $0p_{3/2}0p_{1/2}$  shells. As an example, for eight major shells we could have  $14\hbar\omega$   $2p - 2h$  excitations from the  $0s_{1/2}$  shell whereas from the  $0p_{3/2}0p_{1/2}$  shell we can at most have  $12\hbar\omega$   $2p - 2h$  excitations. The latter fixes the total number of allowed excitations with eight major shells for  ${}^{16}\text{O}$ . The fact that the energies seem to converge at this level of truncation is a welcome feature which can be exploited in the coupled-cluster calculations. These calculations, see below, are much more challenging from a computational point of view since we in principle generate a much larger class of diagrams. In this work we are limited to computations with at most seven major shells in helium and six major shells in oxygen in our coupled-cluster calculations. This means that hopefully the trend seen in Figs. 4 and 5 allows us to limit our coupled-cluster calculations to six or seven major shells. Secondly, although the minimum shifts a little as function of the oscillator energy as we increase the oscillator space, we notice that as the number of major shells is increased, the dependence of the binding energy upon the oscillator parameter weakens. A similar feature is seen in the coupled-cluster calculations below. For  ${}^{16}\text{O}$  the minimum for seven shells takes place at  $E/A = -7.155$  MeV for  $\hbar\omega = 12.9$  MeV and for eight shells we have  $E/A = -7.120$  MeV at  $\hbar\omega = 13.6$  MeV.

For six shells we obtain  $E/A = -7.416$  MeV at  $\hbar\omega = 12.6$  MeV. The curvature for larger values of  $\hbar\omega$  decreases with increasing number of shells  $N$ . At  $\hbar\omega = 18$  MeV we have for  $^{16}\text{O}$  and  $N = 8$  that  $d(E/A)/d\omega = 0.217$ , for  $N = 7$  we obtain  $d(E/A)/d\omega = 0.277$  and  $N = 6$  we have  $d(E/A)/d\omega = 0.346$ . The corresponding derivatives for  $^4\text{He}$  at  $\hbar\omega = 18$  MeV are for  $N = 8$   $d(E/A)/d\omega = 0.119$ , for  $N = 7$   $d(E/A)/d\omega = 0.158$  and for  $N = 6$   $d(E/A)/d\omega = 0.209$ , indicating a smoother dependence upon  $\hbar\omega$  with increasing  $N$ . The reader should also note that in the limit  $\hbar\omega \rightarrow 0$  we have  $E \rightarrow 0$ . Finally, we observe that we are not able to reproduce the experimental binding energies. We will come back to this point in Sec. V where a comparison with coupled cluster theory is also made.

#### IV. COUPLED CLUSTERS IN SINGLE AND DOUBLE EXCITATIONS

In this section, we will discuss a formal derivation of the coupled-cluster equations. While this discussion is standard in quantum chemistry (see, for example Ref. [6]), the nuclear physics community may not be familiar with this formulation of coupled-cluster theory. We will therefore introduce notations and equations that we will continue to use throughout our discussion (in this and following papers) of this technique and its extensions.

We must first bring the Hamiltonian into normal ordered form with respect to the reference state  $|\Psi_0\rangle$ . The Hamiltonian then becomes

$$H_{\text{eff}}(\omega) = t + G(\omega) = \sum_{pq} f_{pq} \{a_p^\dagger a_q\} + \frac{1}{4} \sum_{pqrs} \langle pq || rs \rangle \{a_p^\dagger a_q^\dagger a_s a_r\} + \langle \Psi_0 | H_{\text{eff}}(\omega) | \Psi_0 \rangle = H_N + E_0, \quad (21)$$

where  $E_0 = \langle \Psi_0 | H_{\text{eff}}(\omega) | \Psi_0 \rangle$  and the Fock-matrix element is given by

$$f_{pq} = \langle p | t | q \rangle + \sum_i \langle pi || ri \rangle. \quad (22)$$

To simplify notation, we will use  $\langle pq || rs \rangle = \langle pq | G(\omega) | rs \rangle$ . We employ bracket notation  $\{ \}$  to indicate normal ordering with respect to the reference state. As stated previously, we use the notation that  $p, q, r, s$  refers to all single-particle states and  $i, j, k, l$  index all sums below the fermi surface. In addition we let  $a, b, c, d$  index all sums above the fermi surface. The total number of single-particle states in the model space is  $N_s = N_p + N_h$  where  $N_p$  refers to the number of particle states, and  $N_h$  is the number of hole states. Hereafter we simply use  $H$  for  $H_{\text{eff}}(\omega)$ .

Formally, the coupled-cluster method begins by postulating that the correlated many-body wave function is given by

$$|\Psi\rangle = \exp(T) |\Psi_0\rangle, \quad (23)$$

where we define the the correlation operator as

$$T = T_1 + T_2 + T_3 + \dots + T_A. \quad (24)$$

The correlation operators are defined in terms of  $n$ -particle  $n$ -hole ( $np$ - $nh$ ) excitation amplitudes as

$$T_1 = \sum_{i < \varepsilon_f, a > \varepsilon_f} t_i^a a_a^\dagger a_i, \quad (25)$$

$$T_2 = \sum_{i, j < \varepsilon_f; ab > \varepsilon_f} t_{ij}^{ab} a_a^\dagger a_b^\dagger a_j a_i, \quad (26)$$

and higher order terms for  $T_3$  to  $T_A$ . Coupled-cluster theory may thus be hierarchically improved upon by increasing the number of  $T_i$  operators one computes. We will call the theory in which only  $T_1$  and  $T_2$  operators are present, CCSD, or coupled-clusters at the single and double excitation level. CCSDT means that  $T_3$  is retained in the correlation operator, while CCSDTQ refers to keeping both  $T_3$  and  $T_4$  correlation operators. In this uncoupled representation, the correlation amplitudes must obey the fermion-symmetry relations which for the  $T_2$  correlation operators yield  $t_{ij}^{ab} = -t_{ji}^{ab} = -t_{ij}^{ba} = t_{ji}^{ba}$ . We will use the short-hand notation  $t_1$  and  $t_2$  to represent the array of all  $1p$ - $1h$  and  $2p$ - $2h$  operators.

We compute the expectation value of the energy from

$$E = \langle \Psi_0 | \exp(-T) H \exp(T) | \Psi_0 \rangle. \quad (27)$$

Because the energy is computed using projective, asymmetric techniques, an important question concerns the physical reality of the coupled-cluster energy. Quantum mechanics requires that physical observables should be expectation values of Hermitian operators. The coupled-cluster energy expression contains the non-Hermitian operator  $[\exp(-T)H\exp(T)]$ . However, if  $T$  is not truncated, the similarity-transformed operator exhibits an energy-eigenvalue spectrum that is identical to the original Hermitian operator,  $H$ , thus justifying its formal use. From a practical point of view, the coupled-cluster energy tends to follow the expectation value result (if the theory is reformulated as a variational theory), even when  $T$  is truncated.

The correlation energy is quite easy to calculate and is given by



$$E_{\text{corr}} = E - E_0 = \sum_{ia} f_{ia} t_i^a + \frac{1}{4} \sum_{aibj} \langle ij || ab \rangle t_{ij}^{ab} + \frac{1}{2} \sum_{aibj} \langle ij || ab \rangle t_i^a t_j^b. \quad (28)$$

For two-body Hamiltonians, this equation is general and is not restricted to the CCSD approximation since higher-order cluster operators such as  $T_3$  and  $T_4$  cannot produce fully contracted terms with the Hamiltonian and therefore contribute zero to the energy. Higher-order operators can contribute to the energy indirectly through the equations used to determine these amplitudes. The three terms in Eq.(28) are usually referred to as the  $T_1$ ,  $T_2$ , and  $T_1^2$  contributions to the correlation energy.

The equations for amplitudes are found by left projection of excited Slater determinants so that

$$0 = \langle \Psi_i^a | \exp(-T) H_N(T) | \Psi_0 \rangle, \quad (29)$$

$$0 = \langle \Psi_{ij}^{ab} | \exp(-T) H_N(T) | \Psi_0 \rangle. \quad (30)$$

The Baker-Hausdorf relation may be used to rewrite the similarity transformation as

$$\begin{aligned} \exp(-T) H_N(T) &= H_N + [H_N, T_1] + [H_N, T_2] \\ &+ \frac{1}{2} [[H_N, T_1], T_1] + \frac{1}{2} [[H_N, T_2], T_2] \\ &+ [[H_N, T_1], T_2] + \dots \end{aligned} \quad (31)$$

The expansion terminates exactly at quadruply nested commutators when the Hamiltonian contains at most two-body terms, and at six nested commutators when three-body terms are present. We stress that this termination is exact, thus allowing for a derivation of exact expressions for the  $t_1$  and  $t_2$  amplitudes. To derive these equations is straightforward but tedious work. For example, one of the amplitude terms is given by

$$\begin{aligned} \langle \Psi_{ij}^{ab} | (G_N T_1^2 T_2)_c | \Psi_0 \rangle &= \sum_{pqrs} \sum_{kc} \sum_{ld} \sum_{mnef} t_k^c t_l^d t_{mn}^{ef} \\ &\langle \Psi_0 | \{a_i^+ a_j^+ a_b a_a\} \{a_p^+ a_q^+ a_s a_r\} \\ &\{a_c^+ a_k\} \{a_c^+ a_k\} \{a_d^+ a_l\} \{a_e^+ a_f^+ a_n a_m\} | \Psi_0 \rangle, \end{aligned} \quad (32)$$

for which Wick's theorem may be used to calculate the expectation matrix element. Here  $G_N$  is the normal ordered  $G$ -matrix operator, and the subscript  $c$  indicates only connected diagrams enter into the computation of the expectation value.

The  $t_1$  amplitude equations are given by

$$\begin{aligned} 0 &= f_{ai} + \sum_c f_{ac} t_i^c - \sum_k f_{ki} t_k^a + \sum_{kc} \langle ka || ci \rangle t_k^c + \sum_{kc} f_{kc} t_{ik}^{ac} + \frac{1}{2} \sum_{kcd} \langle ka || cd \rangle t_{ki}^{cd} \\ &- \frac{1}{2} \sum_{klc} \langle kl || ci \rangle t_{kl}^{ca} - \sum_{kc} f_{kc} t_i^c t_k^a - \sum_{klc} \langle kl || ci \rangle t_k^c t_l^a + \sum_{kcd} \langle ka || cd \rangle t_k^c t_i^d \\ &- \sum_{klcd} \langle kl || cd \rangle t_k^c t_i^d t_l^a + \sum_{klcd} \langle kl || cd \rangle t_k^c t_l^d t_i^a - \frac{1}{2} \sum_{klcd} \langle kl || cd \rangle t_{ki}^{cd} t_l^a - \frac{1}{2} \sum_{klcd} \langle kl || cd \rangle t_{kl}^{ca} t_i^d. \end{aligned} \quad (33)$$

This equation is non-linear in the  $t_1$  amplitudes, and linear in the  $t_2$  amplitudes.

The  $t_2$  amplitude equations are given by

$$\begin{aligned} 0 &= \langle ab || ij \rangle + \sum_c (f_{bc} t_{ij}^{ac} - f_{ac} t_{ij}^{bc}) - \sum_k (f_{kj} t_{ik}^{ab} - f_{ki} t_{jk}^{ab}) \\ &+ \frac{1}{2} \sum_{kl} \langle kl || ij \rangle t_{kl}^{ab} + \frac{1}{2} \sum_{cd} \langle ab || cd \rangle t_{cd}^{ij} + P(ij)P(ab) \sum_{kc} \langle kb || cj \rangle t_{ac}^{ik} \\ &+ P(ij) \sum_c \langle ab || cj \rangle t_i^c - P(ab) \sum_k \langle kb || ij \rangle t_k^a \\ &+ \frac{1}{2} P(ij)P(ab) \sum_{klcd} \langle kl || cd \rangle t_{ik}^{ac} t_{lj}^{db} + \frac{1}{4} \sum_{klcd} \langle kl || cd \rangle t_{ij}^{cd} t_{kl}^{ab} - \frac{1}{2} P(ab) \sum_{klcd} \langle kl || cd \rangle t_{ij}^{ac} t_{kl}^{bd} - \frac{1}{2} P(ij) \sum_{klcd} \langle kl || cd \rangle t_{ik}^{ab} t_{jl}^{cd} \end{aligned}$$

$$\begin{aligned}
& + \frac{1}{2}P(ab) \sum_{kl} \langle kl || ij \rangle t_k^a t_l^b + \frac{1}{2}P(ij) \sum_{cd} \langle ab || cd \rangle t_i^c t_j^d - P(ij)P(ab) \sum_{kc} \langle kb || ic \rangle t_k^a t_j^c \\
& + P(ab) \sum_{kc} f_{kc} t_k^a t_{ij}^{ab} + P(ij) \sum_{kc} f_{kc} t_i^c t_{jk}^{ab} \\
& - P(ij) \sum_{klc} \langle kl || ci \rangle t_k^c t_l^{ab} + P(ab) \sum_{kcd} \langle ka || cd \rangle t_k^c t_{ij}^{db} + P(ij)P(ab) \sum_{kcd} \langle ak || dc \rangle t_i^d t_{jk}^{bc} \\
& + P(ij)P(ab) \sum_{klc} \langle kl || ic \rangle t_l^a t_{jk}^{bc} + \frac{1}{2}P(ij) \sum_{klc} \langle kl || ck \rangle t_i^c t_{kl}^{ab} - \frac{1}{2}P(ab) \sum_{kcd} \langle kb || cd \rangle t_k^a t_{ij}^{cd} \\
& - \frac{1}{2}P(ij)P(ab) \sum_{kcd} \langle kb || cd \rangle t_i^c t_k^a t_j^d + \frac{1}{2}P(ij)P(ab) \sum_{klc} \langle kl || cj \rangle t_i^c t_k^a t_l^b \\
& - P(ij) \sum_{klcd} \langle kl || cd \rangle t_k^c t_l^d t_{ij}^{ab} - P(ab) \sum_{klcd} \langle kl || cd \rangle t_k^c t_l^a t_{ij}^{db} + \frac{1}{4}P(ij) \sum_{klcd} \langle kl || cd \rangle t_i^c t_j^d t_k^a t_l^b \\
& + \frac{1}{4}P(ab) \sum_{klcd} \langle kl || cd \rangle t_k^a t_l^b t_{ij}^{cd} + P(ij)P(ab) \sum_{klcd} \langle kl || cd \rangle t_i^c t_l^b t_{kj}^{ad} + \frac{1}{4}P(ij)P(ab) \sum_{klcd} \langle kl || cd \rangle t_i^c t_k^a t_j^d t_l^b . \tag{34}
\end{aligned}$$

The permutation operator  $P$  yields

$$P(ij)f(ij) = f(ij) - f(ji) \tag{35}$$

The equations of the  $t_2$  amplitudes are nonlinear in both  $t_1$  and  $t_2$  terms. While these equations appear quite lengthy, they are solvable through iterative techniques that we will discuss below. We note that the amplitude equations include terms that allow for  $4p-4h$  excitations. Indeed, while we speak of doubles in terms of amplitudes, the class of diagrams involved in the theory include fourth-order terms. This is a very important difference and distinction between the shell model with up to  $2p-2h$  excitations and CCSD. Furthermore, when the energy is computed in CCSD, all terms are linked and connected.

In order to calculate expectation values of operators we use the Hellmann-Feynman theorem [38] which states that if we perturb our Hamiltonian such that  $H' = H + \lambda\Omega$  where  $\lambda$  is a small quantity and  $\Omega$  is the operator of interest, then the energy changes only by a small amount from its original value of  $E(\lambda = 0)$ . As a function of  $\lambda$ , the energy becomes  $E' = E(\lambda = 0) + \lambda dE/d\lambda$ , and the expectation value of the operator is given by

$$\langle \Omega \rangle = \frac{dE(\lambda = 0)}{d\lambda} . \tag{36}$$

## V. CCSD CALCULATIONS FOR HELIUM AND OXYGEN

### A. Iteration of the equations

Several computational challenges arise when we implement the CCSD equation solver. One problem involves

memory requirements for the  $G$ -matrix, which in its uncoupled form is a 4-index tensor and therefore requires a large amount of storage. In order to maintain fast computation, we do not employ storage compression of the  $G$ -matrix at this stage. Thus, for example, an  $N = 7$  calculation requires 100 GBytes of storage for the  $G$ -matrix elements. Present-day parallel computing systems use distributed memory architectures that allow for the storage of such large sets of data. Our implementation in distributing the  $G$ -matrix is to store the third and fourth indices across processors in sub-matrix blocks. In doing this, we are able to take advantage of the large available memory for storing the matrix elements.

We use an iterative method to generate solutions to the  $t_1$  and  $t_2$  amplitude equations. In this paper, we are concerned with closed shell nuclei. In this case, a slight rearrangement of Eqs. (33) and (34) gives a second order perturbative initial solution for the amplitudes. For the  $t_1$  amplitude, we rearrange the first few terms by pulling out the diagonal in the first two sums and defining a  $1p-1h$  and  $2p-2h$  energy denominators as

$$D_i^a = f_{ii} - f_{aa} , \tag{37}$$

$$D_{ij}^{ab} = f_{ii} + f_{jj} - f_{aa} - f_{bb} . \tag{38}$$

The first terms in the  $t_1$  and  $t_2$  amplitude equations then become

$$D_i^a t_i^a = f_{ai} + \sum_c (1 - \delta_{ca}) f_{ac} t_i^c - \sum_k (1 - \delta_{ik}) f_{ik} t_k^a + \dots, \quad (39)$$

$$D_{ij}^{ab} t_{ij}^{ab} = \langle ab || ij \rangle + P(ab) \sum_c (1 - \delta_{bc}) f_{bc} t_{ij}^{ac} + P(ij) \sum_k (1 - \delta_{kj}) f_{kj} t_{ij}^{ab} + \dots. \quad (40)$$

While these are exactly the same equations as given in Eqs. (33) and (34), we may use them to begin an iterative solution by initially setting all amplitudes on the left-hand side to zero. We then obtain for initial amplitudes

$$t_i^a = \frac{f_{ai}}{D_i^a} \quad (41)$$

$$t_{ij}^{ab} = \frac{\langle ab || ij \rangle}{D_{ij}^{ab}}. \quad (42)$$

We now need to compute the various terms in Eq. (34) to obtain the new amplitudes. Since our  $G$ -matrix elements are distributed across processors, we will have partial sums on certain indices. For clarity, we do not show this complication in the following. We demonstrate the numerical procedure by considering one of the terms in the two-particle-two-hole amplitude equation, Eq. (34):

$$f(ab, ij) = \sum_{kl, cd} \langle kl || cd \rangle t_{ij}^{cd} t_{kl}^{ab} \quad (43)$$

We perform the following mapping to matrices  $M$ ,  $N$ , and  $O$ ,  $P$ , and  $Q$ :

$$\begin{aligned} M_{\alpha, \beta} &= t_{kl}^{ab} \\ N_{\beta, \gamma} &= \langle kl || cd \rangle \\ O_{\gamma, \delta} &= t_{ij}^{cd} \\ Q_{\alpha, \delta} &= f(ab, ij) \end{aligned} \quad (44)$$

where we map the indices  $\alpha = (a, b)$ ,  $\beta = (k, l)$ ,  $\gamma = (c, d)$ , and  $\delta = (i, j)$ . Our computation then becomes two matrix-matrix multiplications:

$$\begin{aligned} P_{\alpha, \gamma} &= \sum_{\beta} M_{\alpha, \beta} N_{\beta, \gamma} \\ Q_{\alpha, \delta} &= \sum_{\gamma} P_{\alpha, \gamma} O_{\gamma, \delta} \end{aligned} \quad (45)$$

followed by a mapping of  $Q_{\alpha, \delta}$  to  $f(ab, ij)$ . All terms in the amplitude equations can be formulated in this way and three important consequences follow. First, the computational work scales from one computation of order  $\mathcal{O}(N_p^4 N_n^4)$  to two computations of  $\mathcal{O}(N_p^4 N_n^2)$ . Second, by formulating the algorithm in this manner, we take advantage of highly optimized Basic Linear Algebra Subprograms (BLAS) [39]. This represents a significant reduction in effort when contrasted with the naive equations. We see that a calculation  $^{16}\text{O}$  should require sixteen times more computational time when compared to

N	$N_s$	$^4\text{He}$	G (in millions)	$^{16}\text{O}$
4	80	1,792	0.93	24,960
5	140	4,000	7.23	77,880
6	224	7,976	40.4	176,240
7	336	14,112	178.5	—

TABLE I: Various memory scalings for the He and O systems as a function of the number of major oscillator shells,  $N$ . Listed are the number of uncoupled single-particle states, the two-particle-two-hole amplitudes in  $^4\text{He}$ , the number of non-zero  $G$ -matrix elements, and the number of nonzero two-particle-two-hole amplitudes in  $^{16}\text{O}$ .

a calculation of  $^4\text{He}$  in the same model space. Due to the longer loop structure in  $^{16}\text{O}$  the time required to complete a single oxygen run is only a factor of ten larger than the He case. Third, because we have sub-blocked the interaction amplitudes, we can spread the work across numerous processors. In doing so, we must perform a global reduction operation (a global sum) in order to generate the new amplitudes for the next iteration. We show in Table I some details of the computational sizes of the  $m$ -scheme problems that we have undertaken in this paper. The number of unknowns for which we are solving is approximately the number of two-particle-two-hole amplitudes. Therefore, in our largest calculation for  $^{16}\text{O}$  we are actually solving approximately 176,300 equations per iteration. We also list the number of nonzero  $G$ -matrix elements in Table I.

Eq. (42) represents the terms that one uses to compute the energy in second-order perturbation theory of the Møller-Plesset type [40]. We show in Table II the energy obtained from the  $0^{\text{th}}$   $E(0)$  iteration and the final iteration  $E(F)$  as a function of increasing oscillator levels in the  $^{16}\text{O}$  system. Note that the difference between the converged CCSD energies and the initial  $0^{\text{th}}$  order energies increases as the basis space increases. The converged summation of the CCSD equations yields approximately 10 MeV (or 0.6 MeV per particle) in extra binding. These findings are corroborated by those from many-body perturbation theory from Sec. III. It is therefore worth comparing these results with those from second-order and third-order many-body perturbation theory as well. These are labeled  $E_{\text{MBPT}}^{2\text{nd}}$  and  $E_{\text{MBPT}}^{3\text{rd}}$  in the same table. The reader should notice that the zeroth iterations of the coupled-cluster schemes already includes corrections to the one-body amplitudes  $t_1$ . However, the energy de-

$N$	$(\hbar\omega)$	$E(0)$	$E_{\text{MBPT}}^{2\text{nd}}$	$E_{\text{MBPT}}^{3\text{rd}}$	$E(F)$
4	14	-135.117	-132.063	-129.920	-140.473
5	14	-124.786	-124.844	-121.520	-127.790
6	14	-121.356	-121.481	-118.233	-119.733

TABLE II: Comparisons of the  $0^{\text{th}}$  order energy  $E(0)$  and the converged CCSD results  $E(F)$  for  $\beta_{c.m.} = 0.0$  in  $^{16}\text{O}$  as a function of increasing model model space. The results are also compared with many-body perturbation theory to second and third order,  $E_{\text{MBPT}}^{2\text{nd}}$  and  $E_{\text{MBPT}}^{3\text{rd}}$ , respectively. All energies are in MeV.

nominators used in the computation of the second-order diagrams of Fig. 3 (diagrams 2 and 3) have hole states determined by Eq. (14). The agreement with the zeroth order iteration and second-order perturbation theory is very good, especially for five and six major shells, as can be seen from Table II. However, for third-order perturbation theory one clearly sees fairly large differences compared with the coupled-cluster results. Typically, the relation between first- and second-order in perturbation theory for  $^{16}\text{O}$  is given by a factor of  $\sim 5 - 6$ . For e.g.,  $N = 5$  and  $\hbar\omega = 14$  MeV, we have  $-329.124$  MeV from first order and  $-47.719$  from second order. To third order we obtain a repulsive contribution of  $3.324$  MeV, to be contrasted with the almost  $3$  MeV of attraction given by higher-order terms in the coupled-cluster expansion. This indicates that many-body perturbation theory to third order is most likely not a converged result. An interesting feature to be noted from many-body perturbation theory calculations is that higher terms loose their importance as the size of system is increased. For  $^4\text{He}$  the relation between first-order and second-order perturbation theory is given by a factor of  $\sim 3 - 4$ , depending on the value of  $\hbar\omega$ . Calculations for  $^{40}\text{Ca}$  not reported here indicate a relation of  $\sim 7 - 9$  between first-order and second-order perturbation theory. This is somewhat expected since the  $G$ -matrix is smaller for larger systems, although the energy denominators becomes smaller.

We show typical convergence curves for our coupled-cluster calculations in Fig. 6 for  $^{16}\text{O}$  for the  $N = 4, 5, 6$  oscillator shell model spaces. In this figure,  $E(I)$  is the energy at the  $I^{\text{th}}$  iteration, while  $E(F)$  is the final energy of the system. We obtain convergence within 50 iterations in most cases. The curves also exhibit an exponentially convergent behavior.

Since the CCSD amplitude equations are nonlinear, we investigated the results obtained by using different initial reference states. The naive choice for  $|\Psi_0\rangle$  is to fill the lowest oscillator states for a given system. For example, we define  $|\Psi_0\rangle$  as the filled  $0s$  state for  $^4\text{He}$  and the filled  $0s-0p$  states for  $^{16}\text{O}$ . This choice is fine for closed shell nuclei since none of the energy denominators discussed above becomes zero, but for other nuclei this would be a problem. As an alternative procedure, we start with the Hartree-Fock ground-state Slater determinant for a given

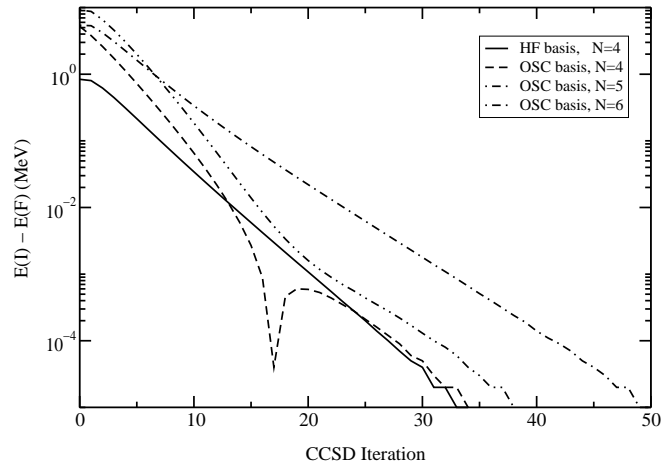


FIG. 6: The convergence of the ground-state energy as a function of the CCSD iterations for  $^{16}\text{O}$ .

system. We solve the Hartree-Fock equations in the oscillator basis in order to obtain transformation matrices  $D$  that take us from the oscillator to the Hartree-Fock basis. We then transform the Hamiltonian to the Hartree-Fock basis using the relation  $a_i^\dagger = \sum_\alpha D_{\alpha i} c_\alpha^\dagger$  where  $a_i$  and  $a_i^\dagger$  annihilate and create particles in the oscillator basis and  $c_\alpha$  and  $c_\alpha^\dagger$  annihilate and create particles in the Hartree-Fock basis. Note that  $D^\dagger D = 1$ . While a complete diagonalization of  $H$  in either basis would yield the same results, the CCSD amplitude equations are not invariant under this transformation since states below and above the fermi surface will be mixed. Furthermore, at the Hartree-Fock level, rotational symmetry of the Hamiltonian is broken, although correlations including those at the CCSD level will restore much of this symmetry. Although we do not discuss in this paper open-shell systems, the Hartree-Fock solution offers a clean way obtain a reference Slater determinant for those cases.

We show in Fig. 6 the convergence of the CCSD equations in both the oscillator and Hartree-Fock basis for  $N = 4$  major shells. In both cases, convergence at the  $10^{-5}$  level is reached before 40 iterations. A more qualitative assessment of how the choice of reference state affects the final results is seen in Table III. In the oscillator basis, the  $1p - 1h$  amplitudes carry a significant fraction of the correlation energy, while in the Hartree-Fock basis these terms do not contribute to the energy. The difference between the Hartree-Fock and oscillator total energies is  $0.6\%$ . We note that if one completely ignores the  $1p - 1h$  amplitudes in the Hartree-Fock basis, the energy becomes  $-138.38$  MeV, a difference of less than  $0.07\%$ . In the oscillator basis, a much larger error of  $5.6\%$  is obtained if one ignores the  $1p - 1h$  amplitudes. Furthermore, the CCD equations (ignoring the  $1p - 1h$  amplitudes) sometimes exhibit numerical instabilities similar to ignoring the Hartree-Fock insertions in many-body perturbation theory discussed above.

Term	Oscillator (MeV)	Hartree-Fock (MeV)
$E_0$	-109.45	-121.977
$T_1$	-9.669	$7 \times 10^{-6}$
$T_1^2$	-1.757	$-0.3 \times 10^{-3}$
$T_2$	-18.439	-16.495
$E_{\text{corr}}$	-29.865	-16.498
$E_{\text{Total}}$	-139.31	-138.47

TABLE III: Comparisons of CCSD results in  $^{16}\text{O}$  when using naively filled oscillator reference state, or when using the Hartree-Fock reference state. These calculations were performed at  $\hbar\omega = 14$  MeV and  $\beta_{\text{c.m.}} = 1.0$ .

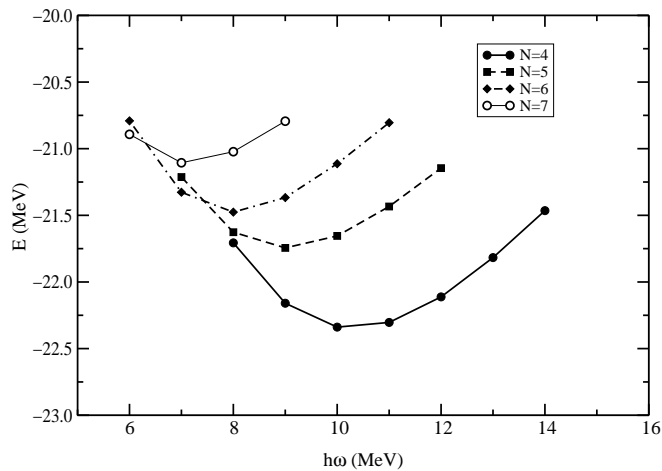


FIG. 7: Dependence of the ground-state energy of  $^4\text{He}$  on  $\hbar\omega$  as a function of increasing model space.

### B. $^4\text{He}$ and $^{16}\text{O}$ ground states

We now return to a discussion of  $^4\text{He}$  and  $^{16}\text{O}$  by providing a description of their ground-state energies using the CCSD formalism. As in the many-body perturbation theory section of this paper, we wish to demonstrate how the coupled-cluster theory converges as a function of increasing model space. We are currently able to perform this study for up to seven major oscillator shells in helium and up to six shells in oxygen. While these studies do not address the starting-energy dependence of the  $G$  matrix, they do indicate the convergence of the calculations as a function of model space, and they indicate the softening of the  $\hbar\omega$  dependence as one moves to larger spaces. The  $\hbar\omega$  dependence of the ground state energy of  $^4\text{He}$  as a function of the model space is shown in Fig. 7 for the  $N = 4, 5, 6, 7$  major oscillator shells with  $\beta_{\text{c.m.}} = 0$ . These curves generally exhibit a parabolic character.

We applied the center-of-mass correction described above to both the He and O nuclei. We demonstrate how this procedure behaves when one solves the CCSD equations in Fig. 8 for  $^4\text{He}$  in the  $N = 4$  and model

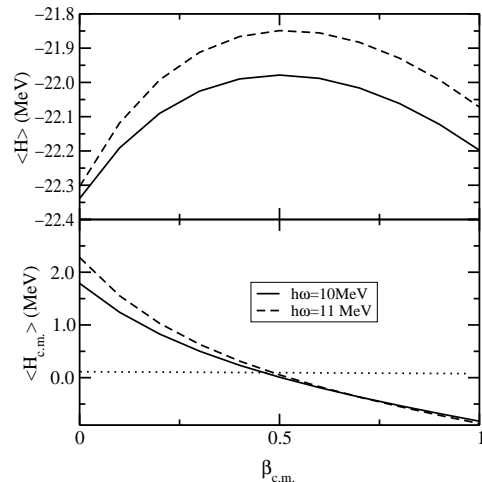


FIG. 8: Top panel: the total energy of  $^4\text{He}$  in four major oscillator shells plotted as a function of the center-of-mass parameter  $\beta_{\text{c.m.}}$ . Bottom panel: the center of mass energy as a function of  $\beta_{\text{c.m.}}$ . The energy is at a variational minimum in this 4 oscillator shell space at  $\hbar\omega = 10$  MeV. The variational minimum for as a function of the CCSD iterations.

space. We calculated the expectation value of  $H_{\text{c.m.}}$  with Eq. (36). These plots indicate that the center-of-mass behavior is less severe when we perform calculations at the variational minimum in  $\hbar\omega$ , which in this case is at  $\hbar\omega = 10$  MeV. We observe that these corrections are rather small for both He and O, amounting to a correction of less than 1% in both cases. This correction only applies to the ground state.

We performed a full diagonalization of  $^4\text{He}$  in four major oscillator shells at  $\hbar\omega = 10$  MeV and  $\beta_{\text{c.m.}} = 0.5$  and obtained an energy of  $-23.4837$  MeV for the ground state as compared to our CCSD result of  $-21.98$  MeV, a 6.8% difference. We anticipate that triples corrections to the energy [41] will recover much of the remaining difference between the complete result and the CCSD result. The CCSD results should be approximately of similar quality in larger model spaces so that we can expect an approximate complete diagonalization energy of  $-22.4$  MeV in seven oscillator shells as compared to  $-21.0$  MeV for the CCSD result. The ground-state energy using Idaho-A was quoted as  $-27.4$  MeV by Navratil and Ormand in Ref. [29]. The major difference between our projected full diagonalization result and  $-27.4$  MeV is most likely due to the differing treatments of the  $G$ -matrix.

In this initial study we performed calculations of the  $^{16}\text{O}$  ground state for up to six major oscillator shells as a function of  $\hbar\omega$ . Fig. 9 indicates the level of convergence of the energy per particle for  $N = 4, 5, 6$  shells. The experimental value resides at 7.98 MeV per particle. While this calculation is not completely converged, it does show signs of convergence as the space is increased. By six oscillator shells, the  $\hbar\omega$  dependence becomes rather minimal. We find a ground-state binding

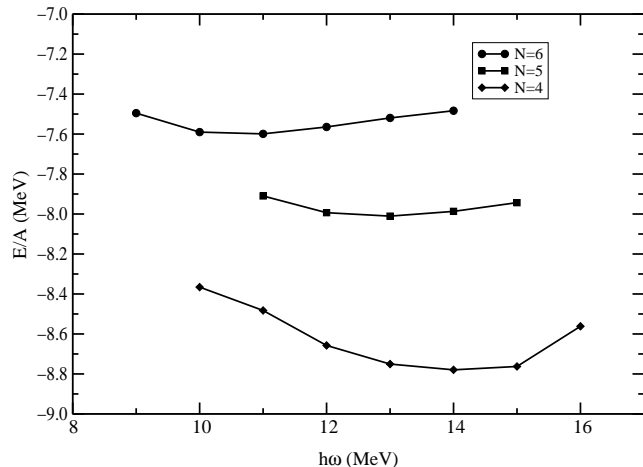


FIG. 9: Dependence of the ground-state energy of  $^{16}\text{O}$  on  $\hbar\omega$  as a function of increasing model space.

energy of 7.6 MeV per particle in oxygen using the Idaho-A potential. Since the Coulomb interaction should give approximately 1 MeV/A of repulsion, and is not included in this calculation, we actually obtain approximately 6.6 MeV of nuclear binding in the 6 major shell calculation which is somewhat above the experimental value. We note that the entire procedure ( $G$ -matrix plus CCSD) tends to approach from below converged solutions.

## VI. CONCLUSIONS AND PERSPECTIVES

Our goal in this paper has been to describe a nonperturbative method of solution to the many-body problem that sums classes of diagrams built upon low order (up to fourth order in this paper) many-body perturbation theory diagrams. We have shown how to calculate nuclear ground states using coupled-cluster methods. In this paper, we concentrated on CCSD equations. We used a  $G$ -matrix as our two-body interaction and we expanded in the spherical harmonic-oscillator basis. We reiterate that CCSD is a nonperturbative approach to the many-body problem: we sum classes of diagrams to infinite order in order to calculate various nuclear properties. The coupled-cluster method discussed here clearly demonstrates the need of summing many-body correlations to infinite order. This is seen when comparing the coupled-cluster results to many-body perturbation theory. Furthermore, the latter is hard to extend beyond third order without a self-consistent single-particle potential and beyond fourth order with a self-consistent potential.

Before closing this paper, we would like to discuss several steps that we will take during the course of this research.

One improvement upon the method will be to include the calculation of triples excitations (called CCSDT or

approximations to it). We indicated that the three-particle-three-hole diagrams likely give repulsion and are important for the description of ground-state properties. Since the CCSD equations do not include the 3p-3h diagrams completely, and since we have seen that these diagrams are important, we will eventually need to include the triples amplitudes into our equations. Various methods that include triples diagrams have been investigated by quantum chemists and we will investigate which of these methods are appropriate for the nuclear problem.

The effort to perform a complete solution to the quantum many-body problem grows exponentially as one adds particles. Combined with the difficulty of methods we suffer in nuclear physics from interactions that are not completely determined. Thus, our methods and techniques for solution typically develop in lock step with our understanding of the nuclear Hamiltonian. While several sets of two-nucleon of interactions that fit nucleon scattering perfectly have been developed over the last 10 years, their many-body characteristics (in particular, their ability to obtain nuclear ground-state masses) indicate that they are insufficient. Three-nucleon interactions become necessary even to fit the triton and  $^4\text{He}$ . To date, no derivations of CCSD (or CCSDT) equations exist that incorporate a three-body interaction. We will pursue this effort in future research.

CCSD and its extensions can be used to obtain excited state information by diagonalizing  $\bar{H} = \exp(-T)H\exp(T)$  in the space of all singly- and doubly-excited determinants where the amplitudes are obtained directly from the converged CCSD amplitudes. This will be an important step in the development of the coupled-cluster method for nuclear science.

Finally, our results do depend on the starting energy of the effective interaction. For  $^{16}\text{O}$  and four oscillator shells and  $\hbar\omega = 14$  MeV, our  $\beta_{\text{c.m.}} = 0.0$  result is  $-140.47$  MeV with the starting energy of  $-80$  MeV, while we obtain  $-143.53$  MeV with a starting energy of  $-60$  MeV. The dependence is therefore weak, but still present. The dependence is more crucial in helium since the binding energy is much lower, and our  $G$ -matrix is not defined for positive starting energies. There are two possible ways to overcome this problem. One is to use the similarity transformation of Lee and Suzuki, following closely the no-core approach of Barrett, Navratil and co-workers [26, 27, 28]. This yields a hermitian and starting energy independent interaction for a large space. Alternatively, one can compute self-consistently the single-particle energies using a  $G$ -matrix defined for both positive and negative starting energies. Thereafter, a starting energy independent interaction can be obtained using e.g., the prescription of Eq. (15), but for both holes and particles. These approaches will be investigated in future works.

### Acknowledgments

Research sponsored by the Laboratory Directed Research and Development Program of Oak Ridge National Laboratory (ORNL), managed by UT-Battelle, LLC for

the U. S. Department of Energy under Contract No. DE-AC05-00OR22725 and the Research Council of Norway. We are pleased to acknowledge useful discussions with David Bernholdt, Ray Bishop, Karol Kowalski, Thomas Papenbrock, Piotr Piecuch, and Neils Walet.

- 
- [1] F. Coester, Nucl. Phys. **7**, 421 (1958).  
 [2] F. Coester and H. Kummel, Nucl. Phys. **17**, 477 (1960).  
 [3] F. Harris, H. Monkhorst, and D. Freeman, *Algebraic and Diagrammatic Methods in Many-Fermion Theory* (Oxford Press, New York, 1992).  
 [4] H. Kummel, K. Luhrmann, and J. Zabolitzky, Phys. Rep. **36**, 1 (1978, and references therein).  
 [5] R. Bartlett, Ann. Rev. Phys. Chem. **32**, 359 (1981).  
 [6] T. Crawford and H. Schaefer III, Reviews in Computational Chemistry **14**, 33 (2000).  
 [7] P. Piecuch, P.-D. Fan, K. Jedziniak, and K. Kowalski, Phys. Rev. Lett. **90**, 113001 (2003).  
 [8] T. Helgaker, P. Jørgensen, and J. Olsen, *Molecular Electronic Structure Theory. Energy and Wave Functions* (Wiley, Chichester, 2000).  
 [9] J. Arponen, Phys. Rev. A **55**, 2686 (1997).  
 [10] I. Lindgren and J. Morrison, *Atomic Many-Body Theory* (Springer, Berlin, 1985).  
 [11] B. Mihaila and J. Heisenberg, Phys. Rev. Lett. **84**, 1403 (2000).  
 [12] B. Mihaila and J. Heisenberg, Phys. Rev. C **61**, 054309 (2000).  
 [13] B. Mihaila and J. Heisenberg, Phys. Rev. C **60**, 054303 (1999).  
 [14] J. Heisenberg and B. Mihaila, Phys. Rev. C **59**, 1440 (1999).  
 [15] I. Moliner, N. Walet, and R. Bishop, J. Phys. G **28**, 1209 (2002).  
 [16] M. Hjorth-Jensen, T. Kuo, and E. Osnes, Phys. Rep. **261**, 125 (1995).  
 [17] R. Machleidt, Phys. Rev. C **63**, 024001 (2001).  
 [18] R. Wiringa, V. Stoks, and R. Schiavilla, Phys. Rev. C **51**, 38 (1995).  
 [19] V. Stoks, R. Klomp, C. Terheggen, and J. de Swart, Phys. Rev. C **49**, 2950 (1994).  
 [20] D. Entem and R. Machleidt, Phys. Lett. B **524**, 93 (2002).  
 [21] S. Weinberg, Phys. Lett. B **363**, 288 (1990).  
 [22] U. van Kolck, Prog. Part. Nucl. Phys. **43**, 337 (1999).  
 [23] D. Entem and R. Machleidt.  
 [24] K. Gad and H. Müther, Phys. Rev. C **66**, 044301 (2002).  
 [25] H. Bethe, B. Brandow, and A. Petschek, Phys. Rev. **129**, 225 (1963).  
 [26] P. Navratil and B. Barrett, Phys. Rev. C **57**, 562 (1998).  
 [27] P. Navratil, J. Vary, and B. Barrett, Phys. Rev. Lett. **84**, 5728 (2000).  
 [28] P. Navratil, J. Vary, and B. Barrett, Phys. Rev. C **62**, 054311 (2000).  
 [29] P. Navratil and W. Ormand, Phys. Rev. Lett. **88**, 152502 (2002).  
 [30] S. Lee and K. Suzuki, Phys. Lett. B **91**, 79 (1980).  
 [31] K. Suzuki and S. Lee, Prog. Theor. Phys. **64**, 2091 (1980).  
 [32] R. R. Whitehead, A. Watt, B. J. Cole, and I. Morrison, Adv. Nucl. Phys. **9**, 123 (1977).  
 [33] R. Lawson, *Theory of the nuclear shell model* (Clarendon Press, Oxford, 1980).  
 [34] D. Dean, M. Ressel, M. Hjorth-Jensen, S. Koonin, K. Langanke, and A. Zuker, Phys. Rev. C **59**, 2474 (1999).  
 [35] T. Papenbrock, A. Juodagalvis, and D. Dean.  
 [36] J. Blaizot and G. Ripka, *Quantum theory of finite systems* (MIT press, Cambridge, USA, 1986).  
 [37] N. Kassis, Nucl. Phys. A **194**, 205 (1972).  
 [38] R. Feynman, Phys. Rev. **56**, 340 (1939).  
 [39] C. Lawson, R. Hanson, D. Kincaid, and F. Krogh, ACM Trans. Math. Soft. **5**, 308 (1979).  
 [40] C. Møller and M. Plesset, Phys. Rev. **46**, 618 (1934).  
 [41] D. Dean, M. Hjorth-Jensen, K. Kowalski, P. Piecuch, and T. Papenbrock, To be published (2003).